SUPPORTING INFORMATION

Multifunctional Theranostic Glyconanoprobes for Synergistic Eradication of Breast Cancer

Gulsah YIGIT ERDEM[a], Beyza GONCU[b], Sezen ATASOY[c], Ayfer YILDIZ UYSAL[d], Serpil DAG[d], and Aydan DAG[e,f*]

[a]Department of Biotechnology, Institute of Health Sciences, Bezmialem Vakif University, 34093, Istanbul, Turkey

[b]Department of Medical Services and Techniques, Vocational School of Health Sciences, Bezmialem Vakif University, 34093, Istanbul, Turkey

[c]Department of Biochemistry, Faculty of Pharmacy, Bezmialem Vakif University, 34093 Istanbul, Turkey

[d]Department of Pathology, Faculty of Veterinary Medicine, Kafkas University, Kars, Turkey

[e]Department of Pharmaceutical Chemistry, Faculty of Pharmacy, Bezmialem Vakif University, 34093, Istanbul, Turkey

[f]Pharmaceutical Application and Research Center, Bezmialem Vakif University, 34093, Istanbul, Turkey

Contents

6. Synthesis of Precursor Compounds

7. Synthesis of Polymers

Synthesis of P(MiMA)-TMS homoblock polymer (P1)

Synthesis of P(MiMA-*b*-DopMA)-TMS diblock copolymer (P2)

Synthesis of P(MiMA-*b*-DopMA-*b*-*ipr*FrMA) triblock copolymer (P3)

Synthesis of azido end functional P(*t*Boc-Lys) (P4)

Synthesis of P(MiMA-*b*-DopMA-*b*-*ipr*FrMA)-b-P(*tBoc*-Lys) polymer via click reaction (P5)

Synthesis of P(MiMA-*b*-DopMA-*b*-FrMA)-*b*-P(Lys) polymer (P6)

Synthesis of Dox conjugated P(MiMA-*b*-DopMA-*b*-FrMA)-*b*-P(Lys) polymer (P-Dox)

8. *In Vitro* Drug Release Study

9. Photothermal Conversion Efficiency of UCNP@MP-Dox

10. Blood Examinations

11. Supplementary Figures and Tables

Figure S1. TEM/EDX analysis of $NaYF_4$:Yb^{3+},Er^{3+}.

Scheme S1: The synthetic pathway of the Dox conjugated glycopeptide polymer, P(MiMA-*b*-DopMA-*b*-FrMA)-*b*-P(Lys)/Dox (P-Dox).

Table S1: Polymerization conditions and molecular weight characteristics of polymers.

Figure S2: ^{1}H-NMR spectra of A) P(MiMA)-TMS (P1), B) P(MiMA-*b*-DopMA)-TMS (P2) and, C) P(MiMA-*b*-DopMA-*b*-*ipr*FrMA)-TMS (P3) (DMSO-d_6).

Figure S3: ^{1}H-NMR spectra of A) P(MiMA-*b*-DopMA-*b*-*ipr*FrMA)-Alk (P3^a), B) P(*tBoc*-Lys) (P4) and, C) P(MiMA-*b*-DopMA-*b*-*ipr*FrMA)-*b*-P(*tBoc*-Lys) (P5) (DMSO-d_6).

Figure S4: ^{1}H-NMR spectra of A) P(MiMA-*b*-DopMA-*b*-FrMA)-*b*-P(Lys) (P6) and, B) P(MiMA-*b*-DopMA-*b*-FrMA)-*b*-P(Lys)/Dox (P-Dox) (DMSO-d_6).

Figure S5: FT-IR spectra of A) P(MiMA)-TMS (P1), P(MiMA-*b*-DopMA)-TMS (P2), P(MiMA-*b*-DopMA-*b*-*ipr*FrMA)-TMS (P3) and, P(MiMA-*b*-DopMA-*b*-*ipr*FrMA)-Alk (P3^a) and B) P(*tBoc*-Lys) (P4), P(MiMA-*b*-DopMA-*b*-*ipr*FrMA)-*b*-P(*tBoc*-Lys) (P5), P(MiMA-*b*-DopMA-*b*-FrMA)-*b*-P(Lys) (P6) and, P(MiMA-*b*-DopMA-*b*-FrMA)-*b*-P(Lys)/Dox (P-Dox).

Figure S6: A) THF-GPC chromatogram of P(MiMA)-TMS (P1), P(MiMA-*b*-DopMA)-TMS

(P2), and P(MiMA-*b*-DopMA-*b*-*ipr*FrMA)-TMS (P3), B) DMF-GPC chromatogram of P(*tBoc*-Lys) (P4) and P(MiMA-*b*-DopMA-*b*-*ipr*FrMA)-*b*-P(*tBoc*-Lys) (P5) and, C) P(MiMA-*b*-DopMA-*b*-FrMA)-*b*-P(Lys)/Dox (P-Dox).

Figure S7: A) UV-Vis absorption spectra of Fe_3O_4 (0.3 mg/mL), UCNP (1.3 mg/mL), Dox (0.025 mg/mL), P-Dox (0.1 mg/mL), UCNP@P-Dox (0.2 mg/mL) and UCNP@MP-Dox (0.25 mg/mL) NPs. B) UV−Vis-NIR spectrum of UCNP@MP-Dox. Dox release profile of C) P-Dox, D) UCNP@P-Dox was measured in different pH buffer solutions (pH 5.5, 6.8, and 7.4) by UV-Vis spectrophotometer.

Figure S8: Agarose gel electrophoresis assay of UCNP@P-Dox/siRNA at various N/P ratios.

Figure S9: Relative cell viability of A-C) 3T3 and D-F) MCF-7 cells after the 24 h and 48 h incubation with different concentrations of UCNP, Polymer (P), P-Dox, and free Dox solutions.

Table S2. IC_{50} values of all MCF7 and 3T3 cells nanoparticles.

Figure S10: FL1-A flow cytometry histograms of 3T3 and MCF-7 cells incubated with 3.9, 7.8, and 15.6 μg/mL concentrations of UCNP, UCNP@P-Dox and Dox in culture media.

Figure S11: Visualization of 3T3 and MCF-7 cells by fluorescence microscopy for cellular uptake after 12 h and 24 h of treated with A) UCNP and B) Dox (scale bar: 100 μm). C) MFI values of 3T3 and MCF-7 cells treated with Dox and UCNP@P-Dox/siRNA after 12 and 24 h.

Figure S12: Relative mRNA expression changes in MCF7 cells after treatment with UCNP@P-Dox and UCNP@P-Dox/siRNA at 7.8 μg/mL concentration. UCNP is abbreviated as U in the graph.

Figure S13: Fluorescence signal (average radiant efficiency) of Dox and UCNP@P-Dox/siRNA at different time points in the tumor.

Figure S14: Biochemistry blood test of liver function parameters (ALT and AST) and kidney function parameters (BUN and CREA) following different treatments of PBS, free Dox and UCNP@P-Dox/siRNA in healthy mice.

Figure S15: Statistical values of Bcl-2 and Bax immunoreactivity score.

Table S3: Statistical Analysis of Mitotic Index Data.

Table S4: Statistical correlation of Bax-Bcl-2 stainings.

1. Materials and methods. Yttrium (III) acetate hydrate (≥99.99%), ytterbium (III) acetate hydrate (≥99.99%), erbium (III) acetate hydrate (≥99.99%), ammonium fluoride (NH_4F, 98%), NaOH (98%), oleic acid (OA, 90%), 1-octadecene (ODE, 90%), iron (III) chloride hexahydrate ($FeCl_3.6H_2O$, ≥99%), sodium oleate (≥99%), 3-bromopropylamine hydrobromide (98%), sodium azide (≥99%, ultradry), potassium hydroxide (95%), magnesium sulfate (≥97%), sodium methoxide (25 wt. % in methanol), dicyclohexylcarbodiimide (DCC, 99%), anhydrous methanol (99.88%), sulfur (99.88%), benzyl chloride (ReagentPlus®, 99%), diethyl ether (≥99.0%), hydrochloric acid (fuming 37%, EMPROVE®), potassium ferricyanide (99%), 4,4'-azobis(4-cyano pentanoic acid) (>98.0%), ethyl acetate (EtOAc, ≥99.7% LC-MS), hexane (for Liquid Chromatography), trimethylsillyl propargyl alcohol (99%), 4-4-(dimethylamino) pyridine (DMAP, purum, ≥98.0%), tetrahydrofuran (THF, for analysis EMSURE® ACS Reagent), sulfuric acid (ACS reagent, 99%), D-fructose (≥99%), acetone (ACS reagent, ≥99.5%), dichloromethane (≥99.8%), pyridine (ACS reagent, ≥99.0%), methacrylic anhydride (≥94%), 3-hydroxytyramine hydrochloride (99%), methacryloyl chloride (97%), triethylamine (Et_3N, ≥99%), *tert*-butyldimethyl sillyl chloride (reagent grade, 97%), 1,8-diazabicyclo[5.4.0]undec-7-ene (DBU, for synthesis), acetonitrile (for liquid chromatography LiChrosolv® Reag. Ph Eur), chloroform (≥99%), chlorotrimethylsilane (≥98.0%), dimethylsulfoxide (DMSO; for analysis ACS), ammonium chloride (NH_4Cl, ACS reagent, ≥99.5%), furfural (for synthesis), *p*-toluenesulfonic acid (ACS reagent, ≥98.5%), benzene (≥99.0%, ACS reagent), ethylene glycol (≥99%), ethanol (EMSURE® Reag. Ph Eur, 96%), ammonium bicarbonate ($NaHCO_3$, ≥99.0%), maleic anhydride (for synthesis), toluene (for analysis EMSURE® ACS, ISO, Reag. Ph Eur), petroleum ether (ACS reagent), ethanolamine (ACS reagent, ≥99.0%), *tert*-butanol (anhydrous, ≥99.5%), di-*tert*-butyl-dicarbonate (ReagentPlus®, 99%), sodium bisulfate (ReagentPlus®, 99%), cyclohexylamine (≥99.9%), N-Boc-L-lysine (≥98%), N,N-dimethylformamide (DMF, ≥99.8%), tetrabutylammonium fluoride (TBAF, 1.0 M in THF), trifluoroacetic acid (≥99), *N,N,N`,N``,N```*-pentamethyldiethylenetriamine (PMDETA, 99%), copper bromide (CuBr, for synthesis) were all from Sigma-Aldrich. 2,2′-Azobis(2-methylpropionitrile) (AIBN, Sigma-Aldrich) was recrystallized twice from methanol (MeOH) and stored at −18 °C. Ultrapure (UP) water was produced by a Milli-Q reverse osmosis system and had a resistivity of 19.6 MΩ·cm. Doxorubicin.HCl were kindly donated by DEVA (Istanbul, Turkey). All solvents for synthesis were obtained from Sigma-Aldrich and used without further purification.

2. Characterization

Nuclear Magnetic Resonance (NMR) Spectroscopy

NMR analyses were conducted using a Bruker BioSpin AG Avance 500 MHz Spectrometer (^{1}H (500 MHz), ^{13}C (125 MHz)). All chemical shifts are expressed in parts per million (ppm) (δ) relative to $Si(CH_3)_4$ as the internal standard (δ = 0 ppm), referenced to the chemical shifts of characteristic solvent signals (^{1}H and ^{13}C).

UV-Vis Spectroscopy

UV-Vis spectra were recorded on a Hitachi U-2900 UV-Vis spectrophotometer.

Fourier-Transform Infrared (FT-IR) Spectroscopy

FT-IR analyses of samples were performed on a Bruker Alpha infrared spectrometer equipped with an attenuated total reflectance (ATR) device and germanium crystal. FT-IR spectra of polymers were recorded within a wave number range of 400-4000 cm^{-1} with a resolution of 4 cm^{-1} from 100 scans in transmission mode. The spectra were determined using both the "OPUS" and Origin v8.5 software.

Gel Permeation Chromatography (GPC)

The molecular weight and polydispersity indices of synthesized polymers were analyzed by gel permeation chromatography (GPC).

THF-GPC analyses were carried out using a Viscotek GPCmax modular system comprising a Viscotek VE 3580 refractive index (RI) detector with HPLC grade THF containing 0.05% 2,6-di*tert*-butyl-4-methylphenol (BHT) eluent system, at a flow rate of 1.0 mL/min on a set of three 300 × 7.8 mm linear columns (T3000, LT4000L, and LT5000L). Polystyrene (PS) or poly(methyl methacrylate) (PMMA) standards were used for calibration and samples were injected using a VE 2001 autoinjector. 50 µL of polymer solution samples with a concentration of 4-5 mg/mL in THF was used for every injection.

DMF-GPC analyses were performed on a TOSOH EcoSEC/GPC system equipped with a refractive index (RI) detector, a UV detector, a DLS Wyatt Dynapro Nanostar detector, and a DAWN HELEOS-18 multi-angle laser light scattering detector, (MALLS detector, Wyatt Technology, Santa Barbara, CA, USA). DMF (0.01 M LiBr, HPLC grade) with a flow rate of 0.5 mL/min at 45 °C was used as the mobile phase. DMF-GPC analyses were performed using serially connected size-exclusion columns (TSKgel HHR guard column, G3000 HHR, and G5000 HHR (7.8 mm ID x 30 cm)). PMMA standards were used for calibration, and molecular

weight and polydispersity indices were determined using either OPUS or TOSOH GPC software.

Dynamic Light Scattering (DLS)

Nanoparticle sizes (the average hydrodynamic diameters and size distributions of the prepared nanoparticle solutions) were determined using a Malvern Zetasizer Nano ZS particle size analyzer equipped with a 4 mV He-Ne laser operating at $\lambda = 632$ nm, an avalanche photodiode detector with high quantum efficiency, and an ALV/LSE-5003 multiple tau digital correlator electronics system. Samples were prepared at a concentration of 1 mg/mL in UP water and purified from dust using a microfilter (0.45 μm) before the measurements.

Transmission Electron Microscopy (TEM)

TEM micrographs were obtained using a JEOL JEM-1400 PLUS transmission electron microscope. The instrument operates at an accelerating voltage of 120.0 kV. Samples were imaged without any staining. The particles were cast onto a carbon-coated copper grid by placing a droplet, a sample solution for 15 min onto its surface. Subsequently, the excess of the solution was removed using filter paper. The grids were dried on air.

3. Synthesis of $NaYF_4$:Yb^{3+}/Er^{3+} Upconversion Nanoparticles (UCNPs). The synthesis of UCNPs was conducted in accordance with the solvothermal synthesis procedure previously established in the literature.[1] In a typical procedure, 0.78 mmol $Y(CH_3CO_2)_3$, 0.20 mmol $Yb(CH_3CO_2)_3$, and 0.02 mmol $Er(CH_3CO_2)_3$ were mixed with 6 mL of oleic acid (OA) and 15 mL of 1-octadecene (ODE) in a 100 mL three-neck round-bottom flask. The resulting mixture was heated to 150 ºC and maintained for 40 min to form a transparent colorless solution and then cooled gradually to room temperature. Subsequently, 10 mL of methanol containing NaOH (0.25 mmol) and NH_4F (4.0 mmol) was added and maintained for 40 min at 50 ºC. After that, the solution was slowly heated to evaporate methanol, degassed at 100 ºC for 10 min, and then heated to 300 ºC and maintained for 90 min under argon atmosphere. After the reaction was finished, the solution was cooled to room temperature. Then, the UCNPs were washed with cyclohexane and ethanol four times to obtain the final $NaYF_4$:Yb^{3+},Er^{3+} nanocrystals, followed by dispersing in cyclohexane. UCNPs were synthesized with a yield of 75%.

4. Synthesis of Magnetic (Fe_3O_4, M) Nanoparticles. Initially, Fe_3O_4 nanoparticles were synthesized using a co-precipitation method[2] involving Fe^{+2} and Fe^{+3} ions in a molar ratio of

1:2. $FeCl_2 \cdot 4H_2O$ (0.6 g, 3.0 mmol) and $FeCl_3 \cdot 6H_2O$ (1.62 g, 6.0 mmol) were dissolved in 10 mL deionized water and kept under the N_2 atmosphere for 20 min. Then, aqueous 25% ammonium hydroxide (NH_4OH) solution (10 mL) was added dropwise (adjusted pH 10) to the mixture under nitrogen gas and stirred vigorously for 30 min at room temperature. The reaction temperature was turned to 80 ºC and it was stirred for another 45 minutes. After the system was cooled to room temperature, the resulting black precipitate was isolated and washed three times with distilled water. Magnetic nanoparticles were separated in an external magnetic field and dried under vacuum. The synthesis of iron oxide nanoparticles resulted in a yield of 78%.

5. Coating Citrate on the UCNPs (UCNP-C). To obtain water-dispersible UCNPs, a ligand exchange procedure was applied following the detailed method described.[3] First, 60 mg of UCNPs were dispersed in 5 mL of hexane. Subsequently, 5 mL of 0.1 M trisodium citrate (pH 4) solution was introduced to the colloidal dispersion of nanoparticles. The mixture was stirred at 700 rpm for 3 h. Then the aqueous/organic system was transferred to the separatory funnel and the aqueous phase containing citrate-coated $NaYF_4$:Yb^{3+},Er^{3+} UCNPs was isolated. The nanoparticles were precipitated with acetone (1:5 aqueous:organic ratio) and centrifuged for 15 min. The organic solvent was removed and the remaining nanoparticles were redispersed in 5 mL of trisodium citrate solution at pH 7 to remove residual oleic acid. The dispersion was stirred for another 2 h. Ultimately, the citrate-coated UCNPs were precipitated with acetone, subjected to three rounds of washing with acetone and water, and gathered through centrifugation. The citrate-coated UCNPs were then dispersed in 2 mL of water for further experiments.

6. Synthesis of Precursor Compounds. 1-Azido-3-amino propane,[4] trimethylsilyl-protected alkyne-functional RAFT agent (CPADB-TMS),[5] 1-*O*-methacryloyl-2,3:4,5-di-*O*-isopropylidene-β-D-fructopyranose (*ipr*FrMA),[6] *N*-(3,4-dihydroxyphenethyl) methacrylamide (DopMA),[7] and *N*-*tert*-butoxycarbonyl-L-lysine-*N*-carboxyanhydride (*tBoc*-Lys-NCA)[8] were synthesized according to published procedures.

Synthesis of 2-(4-formyl-1,3-dioxo-1,3,3a,4,7,7a-hexahydro-2H-4,7-epoxyisoindol-2-yl) ethyl methacrylate

The reaction was carried out in four steps. In the first step, 2-(furan-2-yl)-1,3-dioxolane was synthesized. For this, furfural (50 mmol), p-toluenesulfonic acid (0.25 mmol), and anhydrous magnesium sulfate (50 mmol) were placed in a 100 mL two-necked flask, 50 mL of benzene was added, and then attached to the Dean-Stark adapter. The reaction mixture was placed under

a nitrogen atmosphere. Ethylene glycol (100 mmol) and 10 mL of benzene were added dropwise to the reaction through a dropping funnel. The reaction temperature was then raised to 100°C and stirred overnight. Subsequently, the reaction was brought to room temperature, and $NaHCO_3$ (0.5 mmol) was added to the reaction mixture. After stirring for half an hour, the solution was filtered through a funnel lined with $NaHCO_3$ at the bottom. It was washed three times with dichloromethane (10 mL) and then subjected to two extractions with dichloromethane/deionized water. The organic phase was dried over magnesium sulfate, filtered, and the solvent was evaporated under vacuum. A liquid and dark brown substance was obtained. Vacuum distillation was performed to purify the material. During vacuum distillation, a light yellow precursor was obtained at 0.12 mbar/50 °C, followed by a more viscous, transparent substance at 0.09 mbar/55 °C. (Yield: 3.1 g, 53%). ^{1}H-NMR ($CDCl_3$, 500 MHz): 7.42 (1H), 7.83 (1H), 6.45 (1H), 6.35 (1H), 5.92 (1H), 4.12 (2H), 3.99 (2H), 2.41 (2H). ^{13}C-NMR ($CDCl_3$, 125 MHz): 151.40, 143.21, 110.17, 108.81, 97.71, 65.17.

In the second step 4-(1,3-dioxolan-2-yl)-3a,4,7,7a-tetrahydro-4,7-epoxyisobenzofuran-1,3-dione was synthesized. Under a nitrogen atmosphere, maleic anhydride (84 mmol) was dissolved in toluene (50 mL) in a double-necked flask. Then, the previously synthesized 2-(furan-2-yl)-1,3-dioxolane (70 mmol) was added to the reaction mixture. The temperature was increased to 80 °C and stirred overnight. After the reaction was completed, toluene was removed under vacuum. The remaining dark brown material was successively washed with petroleum ether and diethyl ether to remove the unreacted ketals. (Yield: 12.01, 73%) ^{1}H-NMR ($CDCl_3$, 500 MHz): 6.62 (2H), 5.50-5.43 (2H), 4.15-4.06 (4H), 3.35-3.29 (2H). ^{13}C-NMR ($CDCl_3$, 125 MHz): 169.54, 167.76, 137.55, 136.56, 100.04, 92.91, 82.60, 66.02, 51.71, 48.94.

In the third step 4-(1,3-dioxolan-2-yl)-2-(2-hydroxyethyl)-3a,4,7,7a-tetrahydro-1H-4,7-epoxyisoindole-1,3(2H)-dione was synthesized. The product obtained in the previous step (28 mmol) was transferred to a three-necked flask and dissolved in methanol (100 mL). Ethanolamine (42 mmol) in methanol (30 mL) was added dropwise to the separatory funnel. While the reaction was under nitrogen atmosphere and in an ice bath, ethanolamine was slowly added drop by drop to the solution. After the addition was complete, the reaction mixture was stirred at room temperature for 30 minutes, and then the temperature was raised to 80 °C. The reaction mixture was stirred overnight with a reflux condenser. After the reaction was complete, the solvent was removed under vacuum. The organic phase was dried with magnesium sulfate and extracted twice with dichloromethane/deionized water. Then, the organic solvent was removed under vacuum. A slightly pink and solid product was obtained. (Yield: 4.90 g, 61%).

^{1}H-NMR ($CDCl_3$, 500 MHz): 6.57-6.51 (2H), 5.42-5.36 (2H), 4.12-4.03 (4H), 3.75-3.73 (4H), 3.05-3.01 (2H), 2.37 (-OH, 1H). ^{13}C-NMR ($CDCl_3$, 125 MHz): 176.09, 174.81, 136.87, 136.25, 100.41, 91.80, 81.37, 66.10, 60.27, 50.31, 47.77, 41.83.

In the fourth step 2-(4-(1,3-dioxolan-2-yl)-1,3-dioxo-1,3,3a,4,7,7a-hexahydro-2H-4,7-epoxyisoindol-2-yl)ethyl methacrylate was synthesized. The substance obtained in the previous step (14 mmol) was dissolved in dichloromethane (150 mL) in a three-necked flask. While the reaction was under nitrogen atmosphere, triethylamine (42 mmol) was added. The mixture was then cooled in an ice bath, and dropwise addition of methacryloyl chloride (21 mmol) in 30 mL of dichloromethane in a separatory funnel was carried out. After the addition was complete, the reaction mixture was stirred at room temperature overnight. The next day, the reaction was terminated, and an extraction was performed using dichloromethane/deionized water. The organic phase was dried with magnesium sulfate, and the solvent was removed under vacuum. The product was isolated by column chromatography (silica gel, 60 Å, 70-230 mesh) using an eluent system of ethyl acetate: hexane (1:2). The solvent mixture was evaporated under vacuum, yielding a dark brown viscous product. The material was dissolved in ethyl acetate, precipitated in hexane, and then stored at -18 °C overnight. A white solid product was obtained. (Yield: 4.00 g, 82%). ^{1}H-NMR ($CDCl_3$, 500 MHz): 6.55-6.47 (2H), 6.05-5.54 (2H), 5.35-5.30 (2H), 4.28 (2H), 4.13-3.99 (4H), 3.80 (2H), 3.00 (2H), 1.89 (3H). ^{13}C-NMR ($CDCl_3$, 125 MHz): 175.47, 173.87, 167.04, 136.99, 135.95, 126.22, 100.39, 91.057, 81.44, 66.05, 60.84, 50.35, 47.98, 37.91, 18.24.

7. Synthesis of Polymers

Synthesis of Poly(2-(4-formyl-1,3-dioxo-1,3,3a,4,7,7a-hexahydro-2H-4,7-epoxyisoindol-2-yl) ethyl methacrylate) Homopolymer (P(MiMA)-TMS) (P1)

P(MiMA) was prepared via RAFT polymerization by using CPADB-TMS. 2 g of MiMA (6.55 mmol, 40 eq.), 0.003 mg of AIBN (18.3 μmol, 0.125 eq.) and 0.055 mg of CPADB-TMS (0.14 mmol, 1 eq.) were dissolved in 3.547 mL of acetonitrile in a septa-sealed round-bottom flask. The mixture was cooled in an ice bath and degassed with nitrogen for an hour. After purging, the polymer solution was subsequently placed in an oil bath. Following a 9-hour polymerization reaction at 70 °C, the reaction flask was cooled with an ice bath and exposed to oxygen to terminate the homopolymerization. Then, polymer mixture was precipitated in diethyl ether (10-fold excess) two times to remove the unreacted monomers and the RAFT agent. The

synthesized P(MiMA) was dried at 40 °C overnight in a vacuum. The molecular weight of P(MiMA)-TMS was ascertained using ^{1}H-NMR and THF-GPC analysis.

Synthesis of Poly(2-(4-formyl-1,3-dioxo-1,3,3a,4,7,7a-hexahydro-2H-4,7-epoxyisoindol-2-yl) ethyl methacrylate-*b*-*N*-(3,4-dihydroxyphenethyl) methacrylamide) Diblock Copolymer (P(MiMA-*b*-DopMA)-TMS) (P2)

The previously obtained P(MiMA)-TMS, which was used as a macro-RAFT agent (0.5 g, 0.094 mmol, $M_{n,NMR}$= 5.10 kDa, 1 eq.), 1.43 g of DopMA (6.46 mmol, 35 eq.), 0.84 mg of AIBN (5.12 μmol, 0.135 eq.), and 3.244 mL of acetonitrile were added in a septa-sealed round-bottom flask. Subsequently, the reaction flask was purged with nitrogen for an hour and placed in an oil bath at 70 °C for 8.5 h. The synthesized P(MiMA-*b*-DopMA) was precipitated twice in diethyl ether to remove the unreacted monomer. Finally, the purified polymer was dried in a vacuum at 40 °C overnight. The molecular weight of P(MiMA-*b*-DopMA)-TMS was ascertained using ^{1}H-NMR and THF-GPC analysis.

Synthesis of Poly(2-(4-formyl-1,3-dioxo-1,3,3a,4,7,7a-hexahydro-2H-4,7-epoxyisoindol-2-yl) ethyl methacrylate-*b*-*N*-(3,4-dihydroxyphenethyl) methacrylamide-*b*- 1-*O*-methacryloyl-2,3:4,5-di-*O*-isopropylidene-β-D-fructopyranose) Triblock Glycopolymer (P(MiMA-*b*-DopMA-*b*-*ipr*FrMA)-Alk) (P3)

Previously synthesized P(MiMA-*b*-DopMA)-TMS was applied as a Macro-RAFT agent to synthesize a triblock copolymer. 2.77 mg of *ipr*FrMA (8.44 mmol, 200 eq.), 0.21 g of P(MiMA-*b*-DopMA)-TMS (35.3 μmol, $M_{n,NMR}$= 5.95 kDa, 1.00 eq.), 0.001 mg of AIBN (7.37 μmol, 0.175 eq.), and the mixture of 3.5 mL of acetonitrile and 3.5 mL toluene were added in a septa-sealed round-bottom flask. Subsequently, the reaction flask was purged with nitrogen for an hour and placed in an oil bath at 70 °C for 8 h. The synthesized P(MiMA-*b*-DopMA-*b*-*ipr*FrMA) was precipitated twice in diethyl ether to remove the unreacted monomer. Finally, the purified polymer was dried in vacuum at 40 °C overnight. The molecular weight of P(MiMA-*b*-DopMA)-TMS was ascertained using ^{1}H-NMR and THF-GPC analysis.

After that, trimethylsilyl protecting groups at the end of P(MiMA-*b*-DopMA-*b*-*ipr*FrMA)-TMS triblock copolymer were removed by hydrolysis reaction in the presence of tetra-n-butylammonium fluoride (TBAF). In a typical procedure, 0.70 g of P(MiMA-*b*-DopMA-*b*-*ipr*FrMA) (20.10 μmol, $M_{n,NMR}$= 34.80 kDa) was dissolved in THF (20 mL). TBAF (0.025 mL, 1 M) solution was added and stirred for 3 h at room temperature under a nitrogen atmosphere

and passed through a neutral aluminum oxide column. After the excess solvent was evaporated and the polymer was precipitated in cold methanol, the purified polymer was dried in a vacuum at 40 °C overnight. The molecular weight of P(MiMA-*b*-DopMA)-TMS was ascertained using ^{1}H-NMR and THF-GPC analysis.

Synthesis of Poly(N-ε-*t*-Butyloxycarbonyl- L-Lysine) (P(*tBoc*-Lys)) (P4)

tBoc-Lys-NCA (1 g) was placed in the pre-dried Schlenk reactor under an argon atmosphere and dissolved by adding 10 mL of dry DMF. After 10 minutes, 500 µL of 1-azido-3-aminopropane (1,36 mmol, 10 mL DMF) was added and stirred under Ar atmosphere at 0 °C for 96 h. After polymerization, DMF was evaporated, and the polymer was dissolved in THF and precipitated in diethyl ether. The white solid polymer was dried under a vacuum at room temperature and stored at -80 °C. The molecular weight of P(*tBoc*-Lys)-N_3 was ascertained using ^{1}H-NMR and THF-GPC analysis.

Synthesis of P(MiMA-*b*-DopMA-*b*-*ipr*FrMA)-*b*-P(*tBoc*-Lys) Polymer via Click Reaction (P5)

0.57 g of P(MiMA-*b*-DopMA-*b*-*ipr*FrMA) (16,4 µmol, $M_{n,NMR}$=34700 g/mol, 1 eq.), 0.116 g of P(*tBoc*-Lys)-N_3 (33.1 mmol, $M_{n,NMR}$=3.50 kDa, 1.1 eq.), 10 µL of PMDETA (45 µmol, 10 eq.), 3 mg of CuBr (22 µmol, 5 eq.), and 6 mL of DMF were added to a Schlenk flask. The mixture was deoxygenated by three freeze-pump-thaw cycles and left under a vacuum. After stirring at 35 °C 48 h, the crude product was passed through a neutral alumina column to remove copper complexes and recovered by precipitation twice in cold methanol. The copolymer was then dialyzed for 48 h (molecular weight cutoff, MWCO 3.5 kDa) against UP water. The residue was collected by lyophilization and elucidated by ^{1}H-NMR measurement.

Synthesis of P(MiMA-*b*-DopMA-*b*-*ipr*FrMA)-*b*-P(*tBoc*-Lys) Polymer (P(MiMA-*b*-DopMA-*b*-FrMA)-*b*-P(Lys)) (P6)

In a general procedure, 0.5 g of P(MiMA-*b*-DopMA-*b*-*ipr*FrMA)-*b*-P(*tBoc*-Lys**)** was dissolved in chloroform: UP water mix (15 mL:2 mL), and then 0.412 mL of TFA was added under nitrogen atmosphere and stirred at room temperature overnight. Subsequently, the solution of hydrolysate was dialyzed for 48 h (MWCO 3.5 kDa) against UP water. Then, the purified P(MiMA-*b*-DopMA-*b*-FrMA)-*b*-P(Lys) tetrablock copolymer was collected by lyophilization and elucidated by ^{1}H-NMR and DMF-GPC measurements.

Synthesis of Dox Conjugated P(MiMA-*b*-DopMA-*b*-FrMA)-*b*-P(Lys) Polymer (P(MiMA-*b*-DopMA-*b*-FrMA)-*b*-P(Lys)/Dox) (P-Dox)

The chemotherapeutic agent, Doxorubicin.HCl (Dox) (20 mg, 1.2 eq. for each aldehyde unit) and tetrablock copolymer (0.1 g, 3.46 mmol) were dissolved in 5 mL of DMSO, and then triethylamine (6 µL) was added and stirred overnight. Subsequently, the Dox-conjugated tetrablock copolymer solution was dialyzed for 48 h (MWCO 3.5 kDa) against UP water. Then, the purified glycopeptide polymer P(MiMA-*b*-DopMA-*b*-FrMA)-*b*-P(Lys)/Dox (P-Dox) was collected by lyophilization and analyzed by ^{1}H-NMR and DMF-GPC measurements.

8. *In Vitro* Drug Release Study. The release profiles of P-Dox polymer (P(MiMA-*b*-DopMA-*b*-FrMA)-*b*-P(Lys)/Dox), UCNP@P-Dox, and UCNP@MP-Dox nanoparticles were performed by the dialysis membrane method in appropriate physiological environments (both acidic pH and neutral pH). For this reason, a release medium with pH 5.5 and 7.4 was prepared, and Dox-loaded nanoparticles (2 mg/2 mL in PBS) were transferred to the dialysis membrane containing 15 mL buffer solution. The substances were mixed in a shaking incubator at 37 °C, and 2 mL samples were taken at specified time intervals for 5 days, and 2 mL of fresh PBS of the same pH was added. Drug release profile was determined by UV-Vis spectrophotometer. The absorbance measurement was conducted at a wavelength of 488 nm, and the efficiency of Dox release was determined through conversion using the equation derived from the Dox standard curve. The identical process was replicated for UCNP@P-Dox and UCNP@MP-Dox.

9. Photothermal Conversion Efficiency of UCNP@MP-Dox. The photothermal conversion efficiency (η) of the UCNP@MP-Dox nanoparticles was determined using the following equations.[9]

$$\eta = \frac{hS(T_{Max} - T_{Surr}) - Q_{Dis}}{I(1 - 10^{-A_{980}})} \qquad (1)$$

The *hS* value in equation 1 is obtained through equation 4 and Figure 2D. Here *h* represents the heat transfer coefficient, and *S* represents the surface area of the container. To calculate the *hS* value, θ value was calculated from eq. 2 and the time constant of heat transfer (τ_s) was found by plotting Figure 2D from eq. 3 using θ value. According to Figure 2D, τ_s was determined to be 279 s. In addition, C_D (4.2 J/°C) represents the heat capacity, and m_D (0.3 g) represents the mass of water in eq. 4. Therefore, according to this equation, the *hS* value was 4.5 mW/°C.

$$\theta = \frac{T - T_{Surr}}{T_{Max} - T_{Surr}} \qquad (2)$$

$$t = -\tau_s \ln(\theta) \quad (3)$$

$$hS = \frac{m_D C_D}{\tau_s} \quad (4)$$

The UCNP@MP-Dox solution reached a maximum constant temperature (T_{Max}) of 51.6 °C, while the environmental temperature (T_{Surr}) stood at 26.5 °C. Therefore, the temperature difference (T_{Max}-T_{Surr}) in the UCNP@MP-Dox solution was 25.1 °C. The laser power (I) is 0.72 W, and the absorbance of the UCNP@MP-Dox at 980 nm (A_{980}) is 0.38. Q_{Dis} represents the heat released due to the absorption of light by the solvent and container. From these calculations, η was determined to be 27%.

10. Blood Examinations. To verify the biosafety of the proposed treatment, healthy athymic female nude mice (NCr nu/nu, 8 weeks old) were randomly assigned to three groups (n=3). They were treated intraperitoneally with PBS, free Dox and UCNP@P-Dox/siRNA. PBS-treated mice were used as a control group. At the end of one week of treatment, the mice were sacrificed, and blood samples were centrifuged at 2000 rpm for 3 minutes to separate the serum, and serum biochemical markers such as alanine aminotransferase (ALT), aspartate aminotransferase (AST), blood urea nitrogen (BUN), and creatinine (CREA) were analyzed.

11. Supplementary Figures and Tables

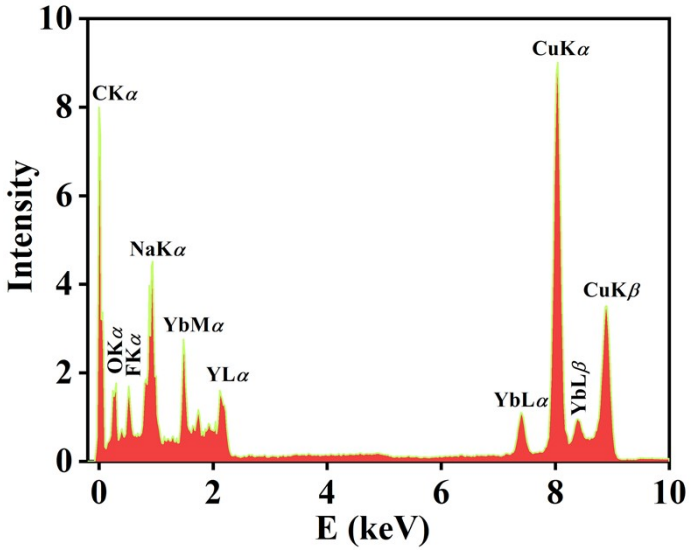

Figure S1. TEM/EDX analysis of $NaYF_4$:Yb^{3+},Er^{3+}.

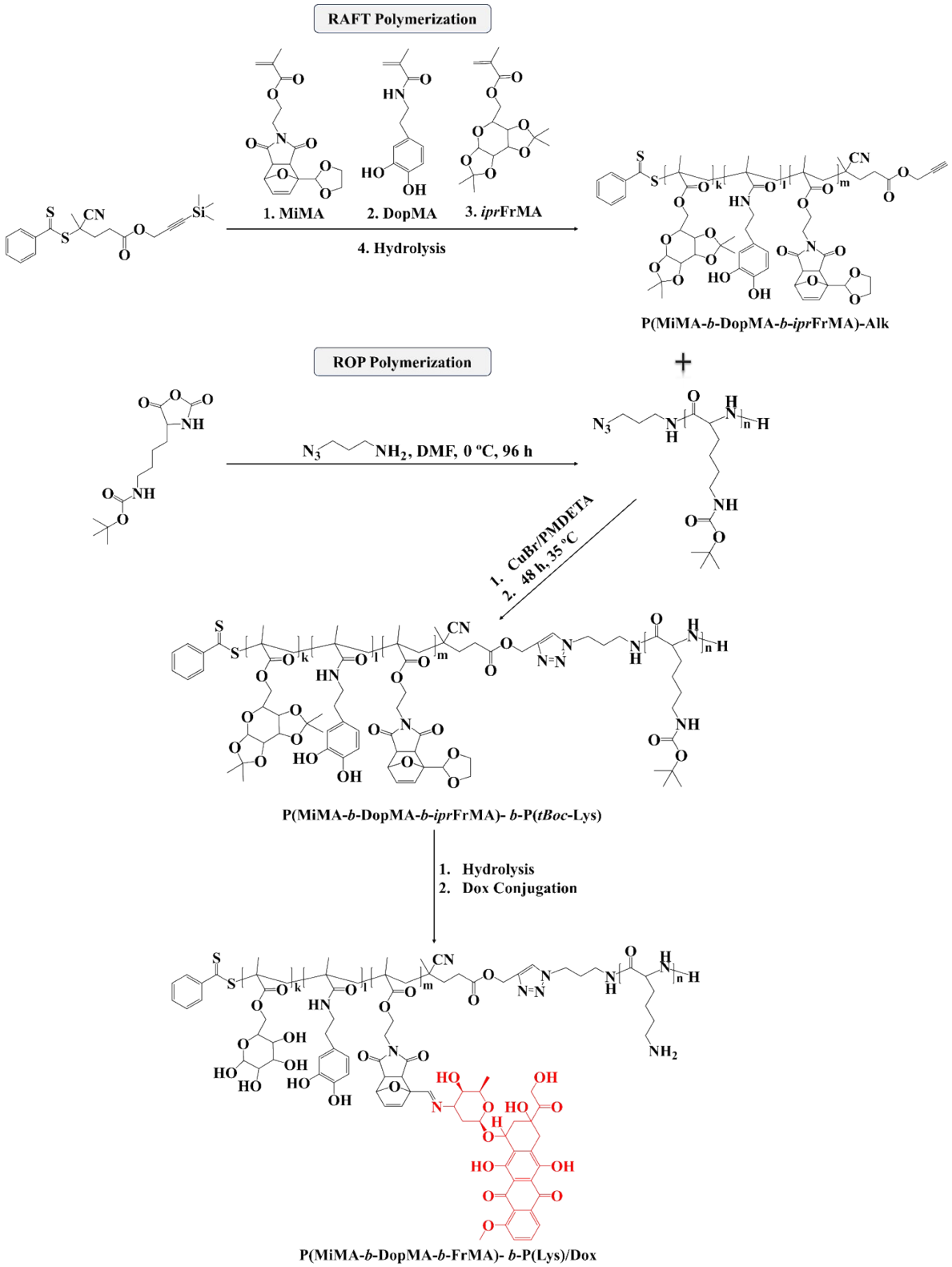

Scheme S1. The synthetic pathway of the Dox conjugated glycopeptide polymer, P(MiMA-*b*-DopMA-*b*-FrMA)-*b*-P(Lys)/Dox (P-Dox).

Code	Polymer	[M]:[RAFT]:[I]	Time (h)	Conv. (%)	$M_{n,NMR}$ (kDa)	$M_{n,GPC}$ (kDa)	M_w/M_n
P1	P(MiMA)$_{14}$-TMS	40:1:0.125	9	35	5.1	2.86[b]	1.35[b]
P2	P(MiMA$_{14}$-*b*-DopMA$_4$)-TMS	35:1:0.135	8.5	12	5.95	3.60[b]	1.36[b]
P3	P(MiMA$_{14}$-*b*-DopMA$_4$-*b*-*ipr*FrMA$_{92}$)-TMS	200:1:0.175	8	46	34.8	42.3[b]	1.38[b]
P3[a]	P(MiMA$_{14}$-*b*-DopMA$_4$-*b*-*ipr*FrMA$_{92}$)-Alk	-	3	>99	34.7	39.9[b]	1.36[b]
P4	P(*tBoc*-Lys)$_{15}$	50:1	96	30	3.5	4.45[c]	1.22[c]
P5	P(MiMA-*b*-DopMA-*b*-*ipr*FrMA)-*b*-P(*tBoc*-Lys)	-	48	>99	38.2	42.5[c]	1.28[c]
P6	P(MiMA-*b*-DopMA-*b*-FrMA)-*b*-P(Lys)	-	18	>99	28.9	32.1[c]	1.36[c]
P-Dox	P(MiMA-*b*-DopMA-*b*-FrMA)-*b*-P(Lys)/Dox	-	18	99	36.3	39.0[c]	1.32[c]

Table S1. Polymerization conditions and molecular weight characteristics of polymers.

[a]After Hydrolysis.
[b]Experimental molecular weights ($M_{n,GPC}$) and polydispersity index (M_w/M_n) were determined by THF-GPC.
[c]Determined by DMF-GPC.

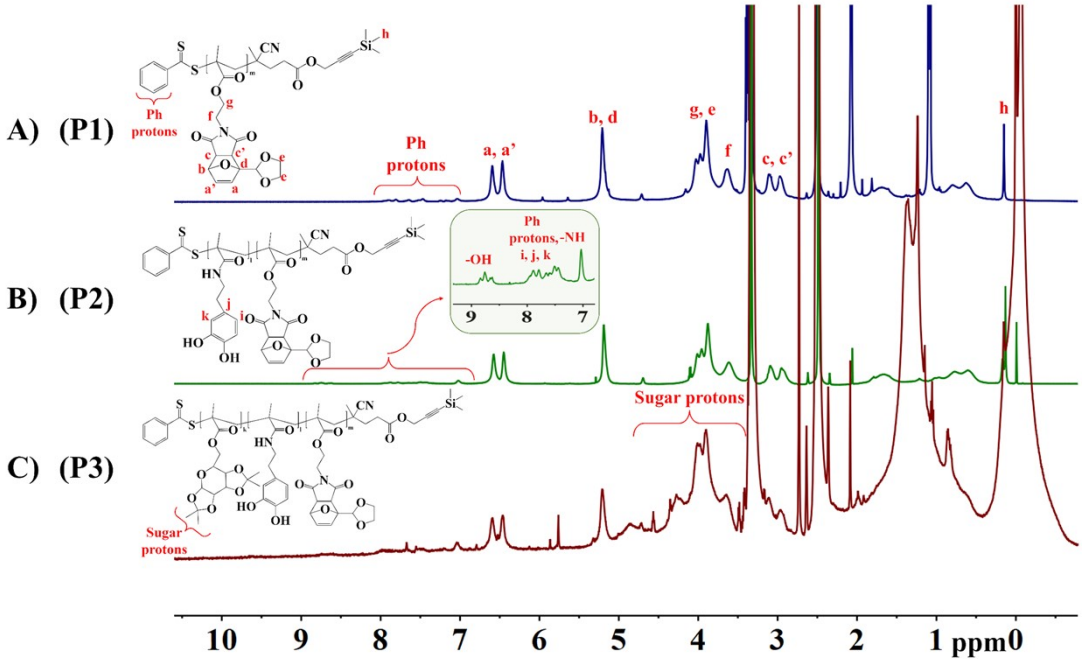

Figure S2. ^{1}H-NMR spectra of **A)** P(MiMA)-TMS (P1), **B)** P(MiMA-*b*-DopMA)-TMS (P2) and, **C)** P(MiMA-*b*-DopMA-*b*-*ipr*FrMA)-TMS (P3) (DMSO-d_6).

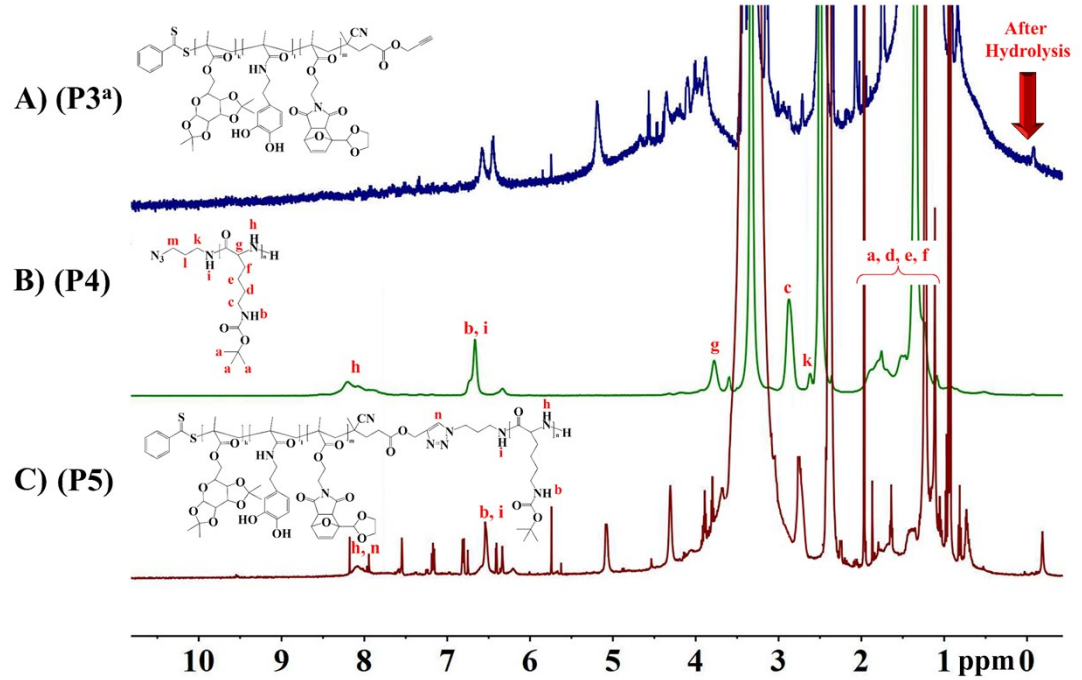

Figure S3. ^{1}H-NMR spectra of **A)** P(MiMA-*b*-DopMA-*b*-*ipr*FrMA)-Alk (P3ª), **B)** P(*tBoc*-Lys) (P4) and, **C)** P(MiMA-*b*-DopMA-*b*-*ipr*FrMA)-*b*-P(*tBoc*-Lys) (P5) (DMSO-d_6).

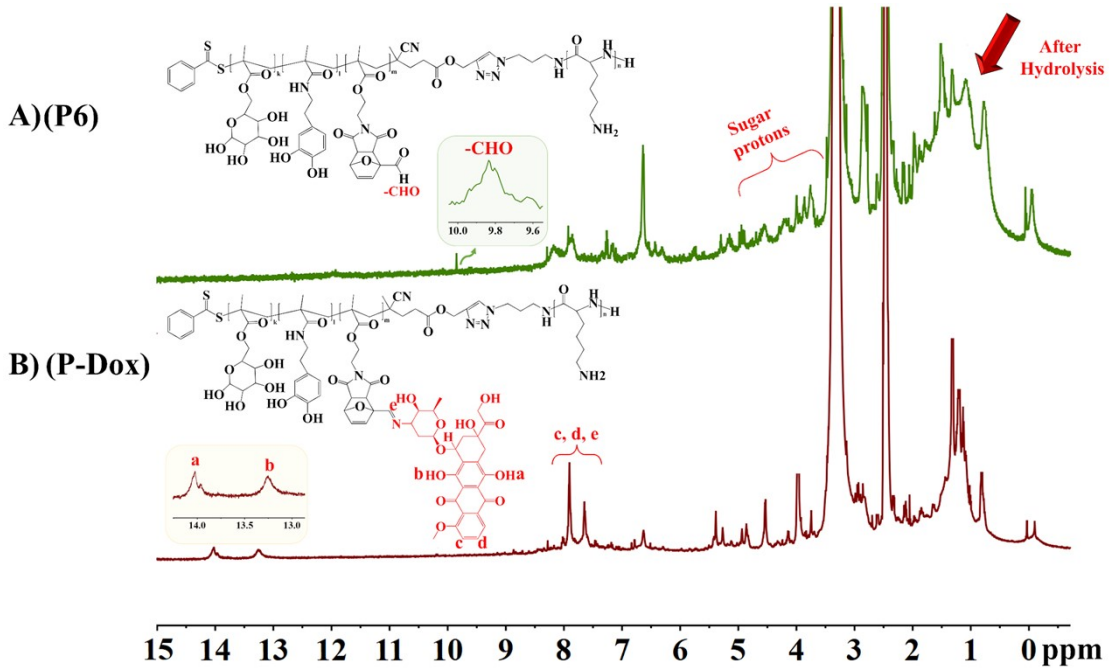

Figure S4. ^{1}H-NMR spectra of **A)** P(MiMA-*b*-DopMA-*b*-FrMA)-*b*-P(Lys) (P6) and, **B)** P(MiMA-*b*-DopMA-*b*-FrMA)-*b*-P(Lys)/Dox (P-Dox) (DMSO-d_6).

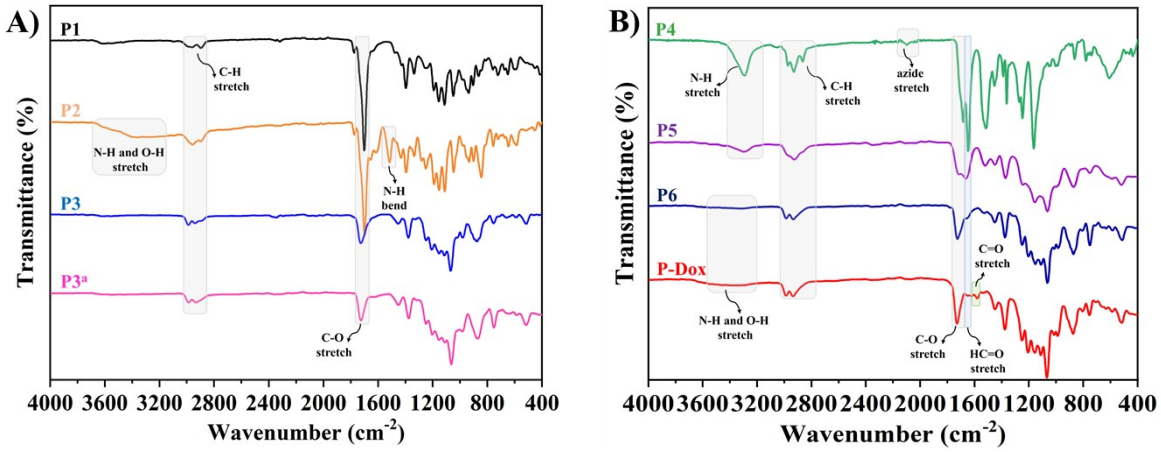

Figure S5. FT-IR spectra of **A)** P(MiMA)-TMS (P1), P(MiMA-*b*-DopMA)-TMS (P2), P(MiMA-*b*-DopMA-*b*-*ipr*FrMA)-TMS (P3) and, P(MiMA-*b*-DopMA-*b*-*ipr*FrMA)-Alk (P3^{a}) and **B)** P(*tBoc*-Lys) (P4), P(MiMA-*b*-DopMA-*b*-*ipr*FrMA)-*b*-P(*tBoc*-Lys) (P5), P(MiMA-*b*-DopMA-*b*-FrMA)-*b*-P(Lys) (P6) and, P(MiMA-*b*-DopMA-*b*-FrMA)-*b*-P(Lys)/Dox (P-Dox).

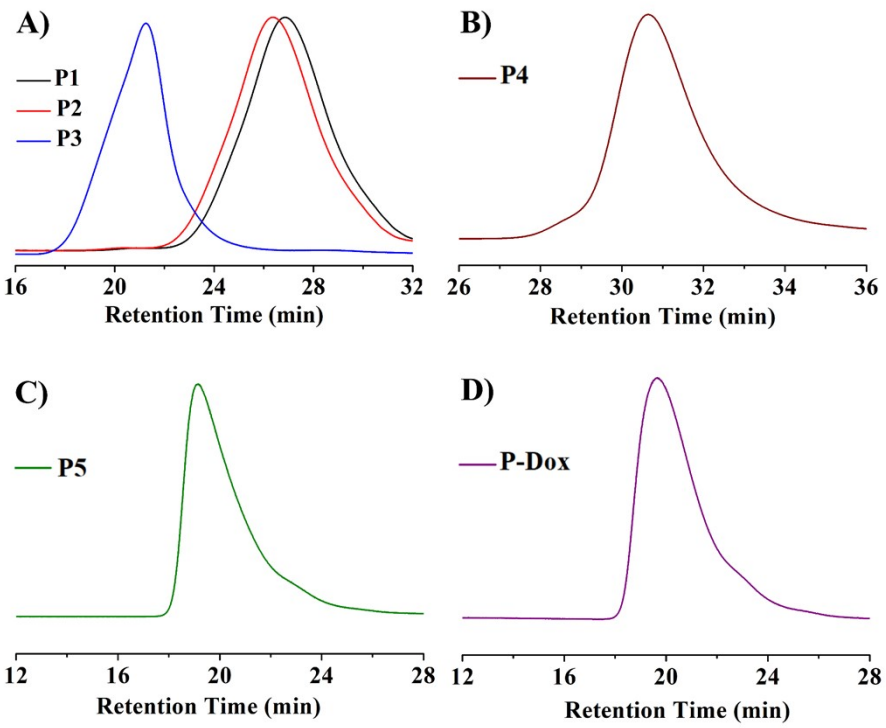

Figure S6. A) THF-GPC chromatogram of P(MiMA)-TMS (P1), P(MiMA-*b*-DopMA)-TMS (P2), and P(MiMA-*b*-DopMA-*b*-*ipr*FrMA)-TMS (P3), **B)** DMF-GPC chromatogram of P(*tBoc*-Lys) (P4) and P(MiMA-*b*-DopMA-*b*-*ipr*FrMA)-*b*-P(*tBoc*-Lys) (P5) and, **C)** P(MiMA-*b*-DopMA-*b*-FrMA)-*b*-P(Lys)/Dox (P-Dox).

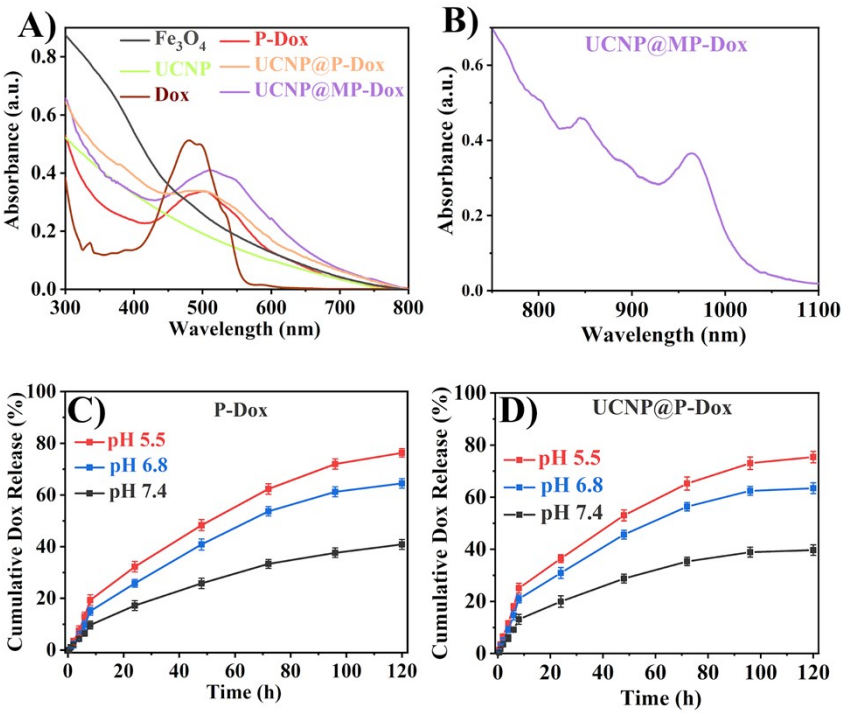

Figure S7. A) UV-Vis absorption spectra of Fe_3O_4 (0.3 mg/mL), UCNP (1.3 mg/mL), Dox (0.025 mg/mL), P-Dox (0.1 mg/mL), UCNP@P-Dox (0.2 mg/mL) and UCNP@MP-Dox (0.25 mg/mL) NPs. **B)** UV−Vis-NIR spectrum of UCNP@MP-Dox. Dox release profile of **C)** P-Dox, **D)** UCNP@P-Dox was measured in different pH buffer solutions (pH 5.5, 6.8, and 7.4) by UV-Vis spectrophotometer.

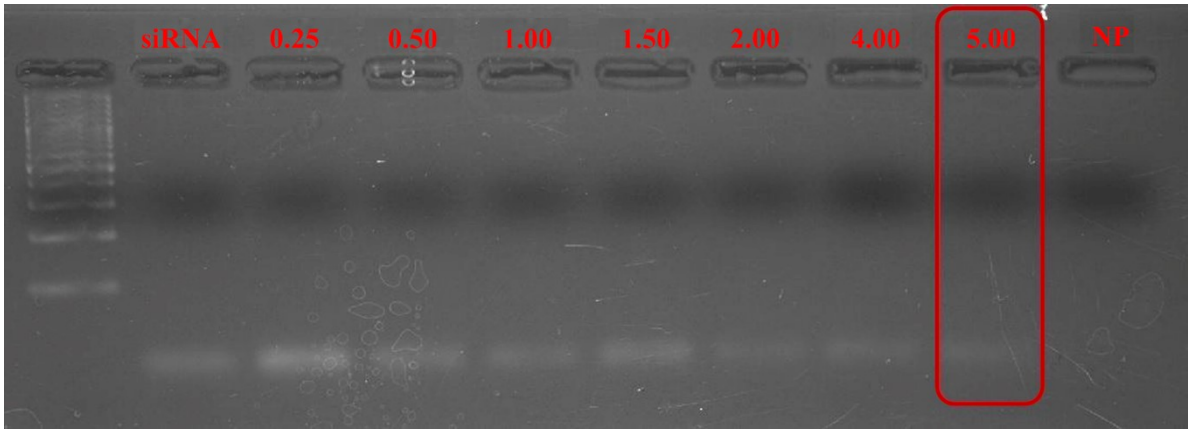

Figure S8. Agarose gel electrophoresis assay of UCNP@P-Dox/siRNA at various N/P ratios.

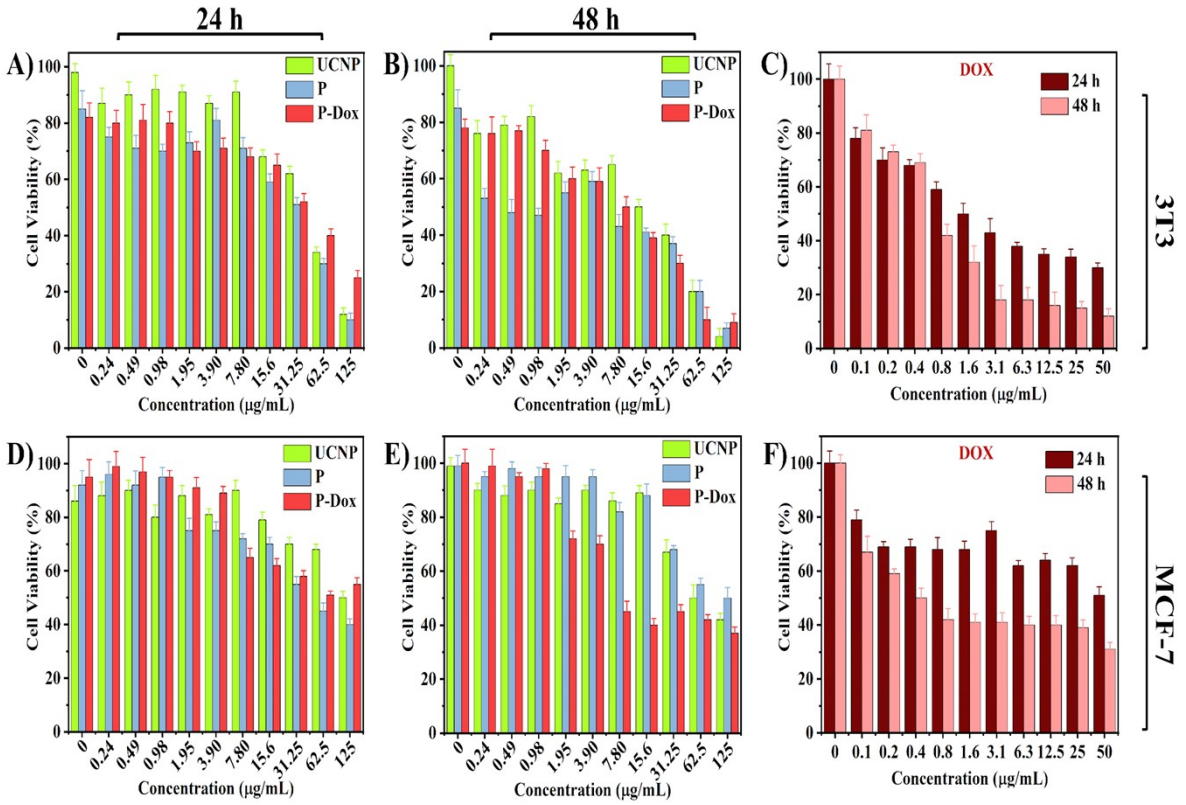

Figure S9. Relative cell viability of **A-C)** 3T3 and **D-F)** MCF-7 cells after the 24 h and 48 h incubation with different concentrations of UCNP, Polymer (P), P-Dox, and free Dox solutions.

Comparison of the viability results from 3-(4,5-dimethylthiazol-2-yl)-2,5-diphenyltetrazolium bromide (MTT) assay. MTT assay was carried out for 24 and 48 h at the indicated concentrations (μg/mL) with UCNP, P, P-Dox, and UCNP@P-Dox/siRNA nanoparticles. Every three independent experiments were performed in triplicates. The result represents the adjusted viability data. Standard deviations from multiple independent experiments were calculated according to the following equation;

$$v = \frac{1}{n-1}\left(\sum_{i=1}^{n} n_i (m_i - m)^2 + \sum_{i=1}^{n} (n_i - 1) v_i\right)$$

In this equation[10];

- n , the total number of experiments,
- m , the total arithmetic mean of all test results,
- m_i , the arithmetic mean of each experimental group,

 v, represents the obtained variances

Table S2. IC_{50} values (µg/mL) of all MCF7 and 3T3 cells nanoparticles. The IC_{50} values were calculated with the following equation by the calculator of AAT Bioquest Inc[1].

$$Y = Min + \frac{Max - Min}{1 + \left(\frac{X}{IC_{50}}\right)^{Hill\ Coefficient}}$$

IC_{50} (µg/mL)	3T3	MCF-7
UCNP	46.25	50.94
P	40.07	37.22
P-Dox	32.43	4.18
UCNP@P-Dox	18.87	33.64
Dox	0.92	0.94

[1] https://www.aatbio.com/tools/linear-logarithmic-semi-log-regression-online-calculator

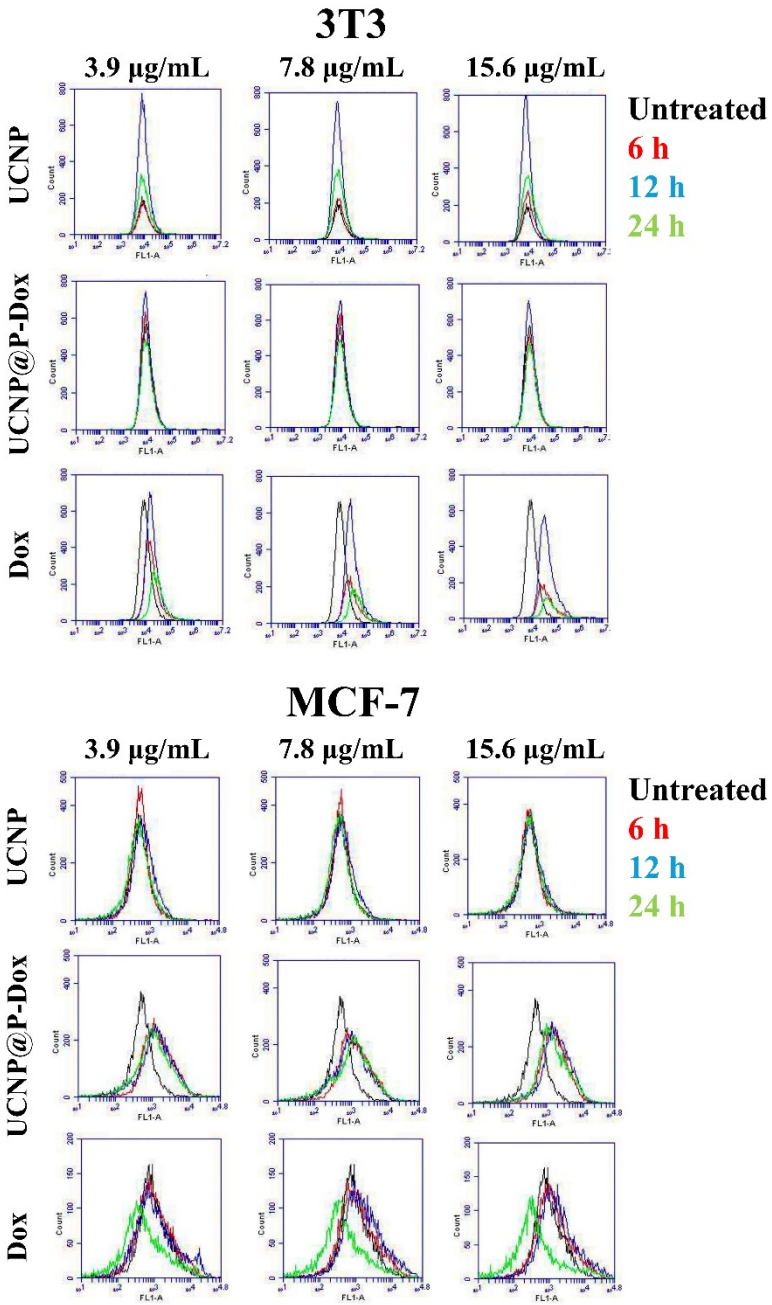

Figure S10. FL1-A flow cytometry histograms of 3T3 and MCF-7 cells incubated with 3.9, 7.8, and 15.6 µg/mL concentrations of UCNP, UCNP@P-Dox, and Dox in culture media. Black, red, blue and green represent untreated, 6, 12, and 24h treated samples.

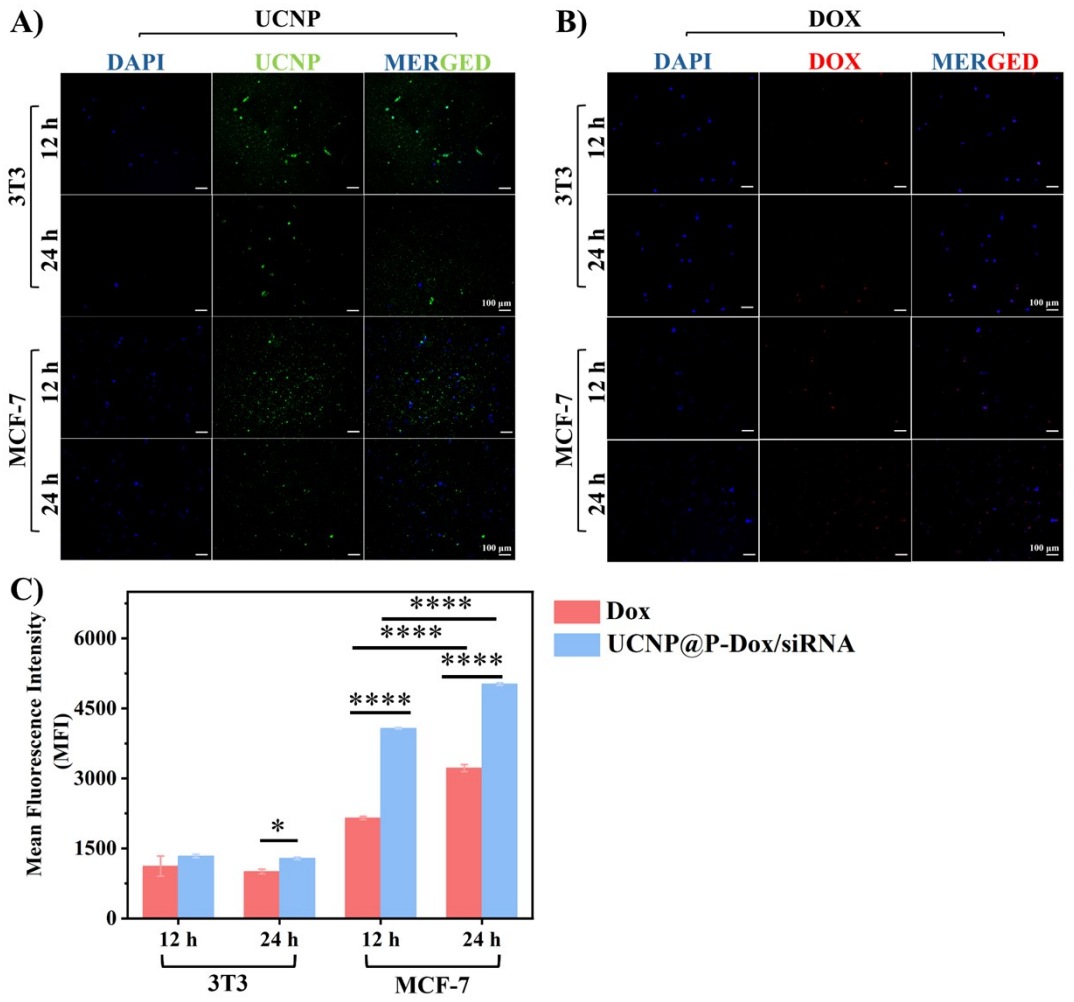

Figure S11: Visualization of 3T3 and MCF-7 cells by fluorescence microscopy for cellular uptake after 12 h and 24 h of treated with **A)** UCNP and **B)** Dox (scale bar: 100 μm). **C)** MFI values of 3T3 and MCF-7 cells treated with Dox and UCNP@P-Dox/siRNA after 12 and 24 h.

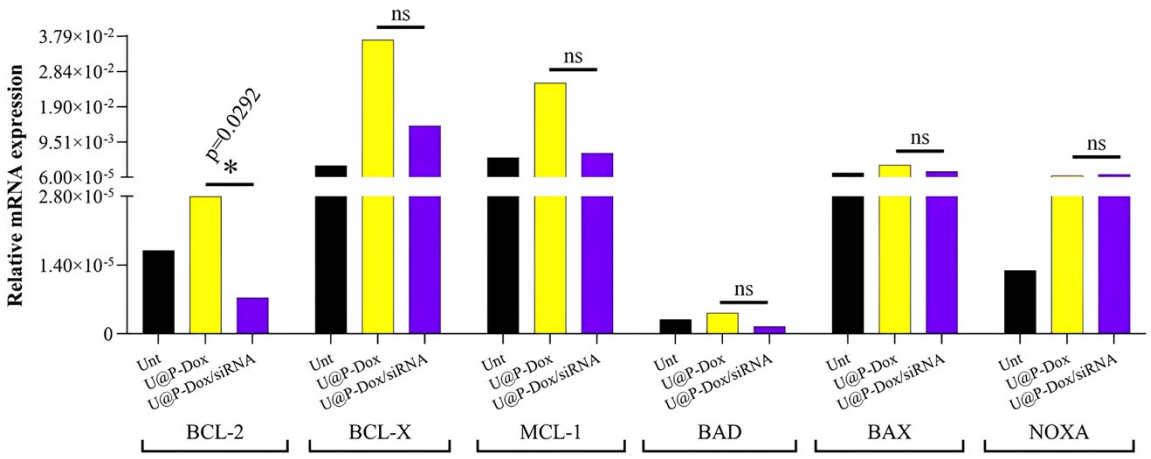

Figure S12. Relative mRNA expression changes in MCF7 cells after treatment with UCNP@P-Dox and UCNP@P-Dox/siRNA at 7.8 µg/mL concentration. UCNP is abbreviated as U in the graph (*p=0.0292).

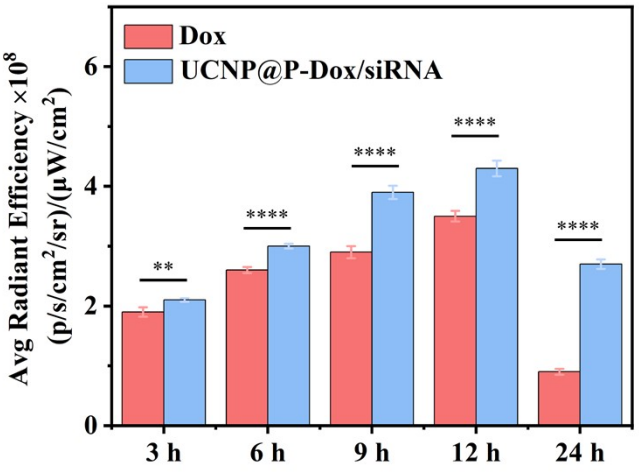

Figure S13. Fluorescence signal (average radiant efficiency) of Dox and UCNP@P-Dox/siRNA at different time points in the tumor (**p<0.01, ****p<0.0001).

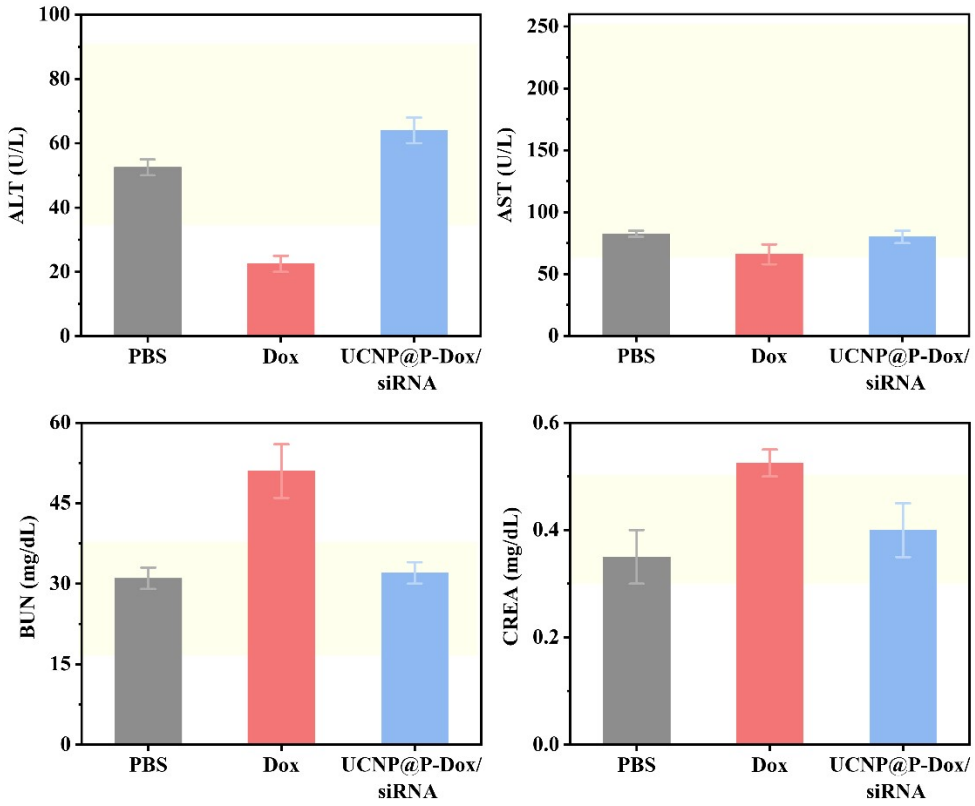

Figure S14. Biochemistry blood test of liver function parameters (ALT and AST) and kidney function parameters (BUN and CREA) following different treatments of PBS, free Dox and UCNP@P-Dox/siRNA in healthy mice.

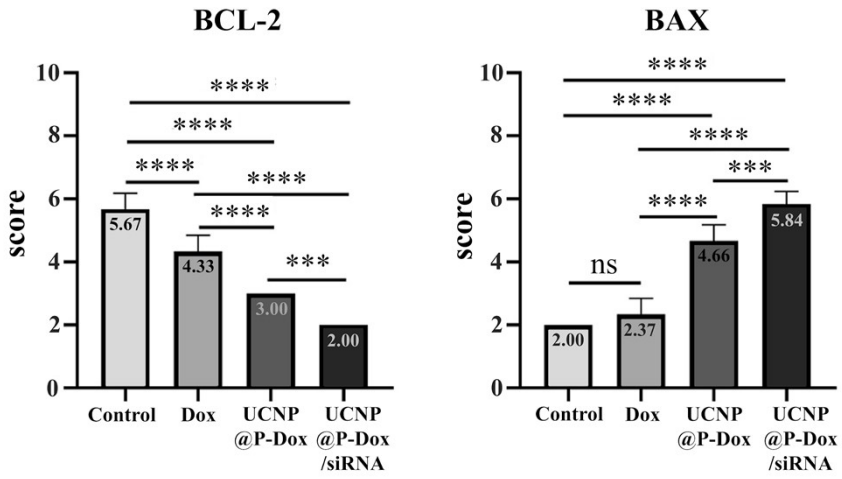

Figure S15. Statistical values of Bcl-2 and Bax immunoreactivity score between the four groups (mean and std. derivation), (***p<0.001, ****p<0.0001).

Table S3: Statistical Analysis of Mitotic Index Data

Group	PCNA	Mitotic index
untreated	401.75±12.49[a]	2.55±0.55[a]
Dox	285±4.95[b]	0.80±0.09[b]
UCNP@P-Dox	218±12.17[c]	0.54±0.12[b]
UCNP@P-Dox/siRNA	192.77±8.13[c]	0.33±0.06[b]
P value	<0.001	<0.002

Footnote: [a-b-c] indicates the statistical difference between groups ($p < 0.05$).

Table S4. Statistical correlation of Bax-Bcl-2 stainings

		Bcl-2	Bax
Bcl-2	Pearson Correlation	1	-,922**
	Sig. (2-tailed)		,000
	N	24	24
Bax	Pearson Correlation	-,922**	1
	Sig. (2-tailed)	,000	
	N	24	24

Correlation is significant at the 0.01 level (2-tailed)

References

1 F. Wang, R. Deng and X. Liu, *Nat Protoc*, 2014, 9, 1634–1644.

2 S. Laurent, D. Forge, M. Port, A. Roch, C. Robic, L. Vander Elst and R. N. Muller, *Chem Rev*, 2008, 108, 2064–2110.

3 R. Naccache, P. Chevallier, J. Lagueux, Y. Gossuin, S. Laurent, L. Vander Elst, C. Chilian, J. A. Capobianco and M. A. Fortin, *Adv Healthc Mater*, 2013, 2, 1478–1488.

4 B. Carboni, A. Benalil and M. Vaultier, *J Org Chem*, 1993, 58, 3736–3741.

5 A. Dag, E. Cakilkaya, P. S. Omurtag Ozgen, S. Atasoy, G. Yigit Erdem, B. Cetin, A. Çavuş Kokuroğlu and A. G. Gürek, *Biomacromolecules*, 2021, 22, 1555–1567.

6 J. Zhao, K. Babiuch, H. Lu, A. Dag, M. Gottschaldt and M. H. Stenzel, *Chem. Commun.*, 2014, 50, 15928–15931.

7 P. Glass, H. Chung, N. R. Washburn and M. Sitti, *Langmuir*, 2009, 25, 6607–6612.

8 J. R. Hernández and H. Klok, *J Polym Sci A Polym Chem*, 2003, 41, 1167–1187.

9 X. Liu, B. Li, F. Fu, K. Xu, R. Zou, Q. Wang, B. Zhang, Z. Chen and J. Hu, *Dalton Transactions*, 2014, 43, 11709.

10 B. Cetin Ersen, B. Goncu, A. Dag and G. Birlik Demirel, *ACS Appl Mater Interfaces*, 2023, 15, 9080–9098.